Journal of Neonatal Surgery
ISSN(Online): 2226-0439
Vol. 14, Issue 32s (2025)
https://www.jneonatalsurg.com

OPEN ACCESS

Arterial Spin Labeling and Dynamic Susceptibility Contrast-Enhanced Perfusion MRI in Evaluation of Adult Patients with Gliomas

Dawlat N. I. Eltatawy[1], Fatma A. Elsharawy[2], Sameh A. Khodair[3], Hanan S. Mahmoud[4], Hanan M. S. El-Ahwal[5]

[1]Assistant lecturer of Radiodiagnosis and Medical Imaging Department, Faculty of Medicine, Tanta University, Tanta, Egypt.
Email ID: Dawleteletatawy@gmail.com

[2]Assistant Professor of Radiodiagnosis and Medical Imaging Department, Faculty of Medicine, Tanta University, Tanta, Egypt.
Email ID: fatma.ahmed@med.tanta.edu.eg

[3]Professor of Radiodiagnosis and Medical Imaging Department, Faculty of Medicine, Tanta University, Tanta, Egypt.
Email ID: sameh.khodair@med.tanta.edu.eg

[4]Professor of Clinical Oncology Department, Faculty of Medicine, Tanta University, Tanta, Egypt.
Email ID: hanan.ali@med.tanta.edu.eg

[5]Professor of Radiodiagnosis and Medical Imaging Department, Faculty of Medicine, Tanta University, Tanta, Egypt.
Email: hanan.elahwal@med.tanta.edu.eg

***Corresponding Author:**
Name: Dawlat N. I. Eltatawy
Affiliation: Assistant lecturer of Radiodiagnosis and Medical Imaging Department, Faculty of Medicine, Tanta University, Tanta, Egypt.
Email ID: Dawleteletatawy@gmail.com

Cite this paper as: Dawlat N. I. Eltatawy, Fatma A. Elsharawy, Sameh A. Khodair, Hanan S. Mahmoud, Hanan M. S. El-Ahwal, (2025) Pathogenesis and Therapeutic Advances in Cholelithiasis: From Gut Microbiota Regulation to the Frontiers of Precision Medicine. *Journal of Neonatal Surgery*, 14 (32s), 293-307.

ABSTRACT

Objectives: To highlight the role of ASL and DSC perfusion MRI in the diagnosis, grading, and follow-up of adult patients with gliomas.

Methods: This prospective study was carried out on 40 patients with MRI features of glioma either for grading or for follow up ,aged from 19 to 68 years old. Non-contrast ASL followed by DSC-PI was done for all cases. The final diagnosis of the cases was established by histopathology.

Results: There was a highly strong correlation between absolute ASL- tumoral cerebral blood flow (tCBF) and absolute DSC -tCBF and DSC-cerebral blood volume (tCBV). ASL- tCBF was significantly different between IDH multiform (GBM) and IDH multiforme (GBM) residual after radiotherapy and chemotherapy. Both ASL and DSCE qualitative color maps showed significant difference between low and high glioma grades. Both ASL-tCBF and ASL –rCBF had sensitivity of 91.9% ,specificity of 90.9 % ,PPV of 91.9% and NPV of 91.9% . DSC-tCBV had sensitivity of 91.6%, specificity of 81.8%, PPV of 84.6% and NPV of 90%.

Conclusions: ASL can serve as a good alternative for dynamic contrast-enhanced perfusion MRI in preoperative grading as well as in follow up of gliomas.

Keywords: *Arterial Spin Labeling, Dynamic Susceptibility Contrast, Magnetic Resonance Imaging, Gliomas*

1. INTRODUCTION

Gliomas account for about 80% of primary brain tumors, with a large variation of 5-year survival rates. [1]

Early symptoms of brain tumors in adults are non-specific, and patients may present multiple times to primary care services before they are referred for investigation. Symptoms include headaches exacerbated by lying down, triggered by the Valsalva maneuver, or associated with vomiting or visual disturbance. [2]

The main diagnostic modality for brain gliomas in general is imaging which mainly includes computed tomography (CT) and conventional magnetic resonance imaging (MRI). [3]

Maximum safe resection of brain gliomas is recommended whenever feasible as its extent is positively correlated with survival. [4] Identification of glioma tissue during surgery is difficult due to its diffuse nature. [5]

CT offers a fast method for the initial diagnosis of brain tissue asymmetry and also is useful for detecting erosion of bony structures as well as the hemorrhagic component of the tumor. [3]

Positron emission tomography (PET) with the amino-acid analogue 3,4-dihydroxy-6-18 F-fluoro-l-phenylalanine (18 F-FDOPA) can be used in the management of primary brain tumors, especially for tumour grading, delineation of tumour extension, treatment planning, treatment response, and post-treatment surveillance. [6]

Conventional MRI enables the assessment of damage to the blood-brain barrier and aids the distinction between benign and malignant brain tumors. [7]

Advanced physiology-based MRI techniques that combine both the spatial localization capabilities of MR imaging with the biochemical and functional information from tissues have been developed for better characterization of brain gliomas, such as MR spectroscopy (MRS), diffusion MRI (dMRI), and perfusion-weighted imaging (PWI) MRI, providing adequate metabolic, structural, and hemodynamic information for treatment planning and monitoring. [5]

PWI techniques have been recently introduced to the pre-operative assessment of gliomas as they can help quantify tumor microcirculation by measuring blood flow and vascular permeability, thus quantifying changes associated with neo-angiogenesis in brain gliomas which is significantly correlated with tumor grades and even provide an important imaging marker for tumor aggressiveness correlating with overall clinical outcomes regardless of histopathological grading. [8, 9]

Arterial spin labelling (ASL) avoids exogenous contrast agents and instead, labels protons in the neck, usually by application of a 180-degree inversion radiofrequency pulse. [10]

The aim of this work was to highlight the role of ASL and dynamic susceptibility contrast (DSC) perfusion MRI in diagnosis, grading, and follow-up of adult patients with gliomas.

2. PATIENTS AND METHODS

This prospective study was carried out on 40 patients aged from 19 to 68 years old, both sexes, with conventional imaging modalities suggestive of brain glioma and pathologically proven brain glioma under treatment. The study was done from August 2022 to August 2024 after approval from the Ethical Committee. Informed written consent was obtained from the patients.

Exclusion criteria were pediatric patients, non-neoplastic parenchymal pathologies such as one case with brain abscess and 12 patients with space-occupying lesions other than gliomas (one case of primary central nervous lymphoma, one case of metastatic brain lesion and ten cases with meningiomas), general contraindications for MRI such as the presence of a cardiac pacemaker or those who have electrically or magnetically activated implants (cochlear implants) and claustrophobic patients, contraindication to contrast media I.V injection such as impaired renal function glomerular filtration rate (GFR) less than 35 mL/min/1.73 m^2, history of allergy to contrast media and no available venous access (three cases).

Patients were divided into two groups: Group A (n=21): pre-operative glioma grading and Group B (n=19): patients with pathologically proven gliomas receiving treatment.

All patients were subjected to complete history taking, general and neurological examination, laboratory investigation [renal function test and GFR], and radiological investigation [brain conventional MRI, ASL, and DSC].

Magnetic resonance imaging

It was performed by using a head coil at MRI unit 1.5 Tesla (GE Signa Explorer), conventional MRI brain imaging protocol with slice thickness was 6 mm, the matrix was 256 x 256, and the field of view was 220-240 mm. All the sequences had the same scan coverage. The scan plane paralleled the line combining anterior and posterior commissure for axial planes, other planes were orthogonally oriented, and the range covered the entire brain. The patient removed metal pins and entered the machine with headfirst in the supine position, foam padding to minimize head motion. Patients were instructed to avoid any head motion during examination time. Its protocol included axial T1 weighted imaging (T1WI) (TR/TE= 400-600/10-20

m/sec). Axial, sagittal, and coronal T2WI (TR/TE=2000-400/100-120 m/sec). Axial fluid-attenuated inversion recovery (FLAIR images) (TR/TE/Inversion time (TI) = 4000-6000/140/1200). High-resolution three-dimensional (3D) T1-weighted spoiled gradient echocardiogram (echo) pulse sequence was acquired; (TR 9.7, TE 4.6, time inversion TI400 ms, flip angle 35°, 124 slices 0.8 mm thick, 208×170 matrix). 3D pseudo-continuous ASL (PCASL) (combines pseudo-continuous (3D-PCASL), and 3D fast spin echo encoding and spiral trajectory acquisition techniques. The parameters for the 3D PCASL sequence were: (TR 4843 ms, TE 10.5 ms; flip angle = 90-degree, slice thickness 2 mm; matrix 64 x64, NEX, 3; FOV 24 × 24 cm2, and interslice space 1 mm). The labeling plane of 3D PCASL was positioned below the scanned volume using a radiofrequency pulse. By applying an amplitude-modulated version of the labeling pulse using a sinusoidal modulation function, blood was alternately tagged and untagged. The total duration of labeling pulses was 2 seconds, with gradient EPI (echo planar) sequence, post label delay 1800 ms. 3D ASL image post-processing using MRI workstation software (ADW 4.7 Vantage, GE Medical Systems). Post-contrast T2 * dynamic susceptibility perfusion with the following parameters: (TR = 1.900 ms, TE = 80 ms, FOV = 30 cm, matrix = 192 x 128, slice thickness = 8 mm without spacing, NEX—1.0). Ten seconds after the start of the image acquisition, a bolus of 1.0 mol/l gadobutrol formula (Gadovist) in a dose of 0.1 ml/kg of body weight was automatically injected with a flow rate of 4 ml/sec, injection was done in the antecubital vein in all cases.

The whole perfusion imaging lasted 1 min 26 s in which sets of images from 13 axial slices were obtained before, during, and after contrast injection. Post-contrast 3D T1-weighted sequence was performed using a contrast bolus administered earlier for the perfusion examination. DSCs enhanced MRI post-processing using MRI workstation software (ADW 4.7 Vantage, GE Medical Systems) at the Radiodiagnosis Department at Tanta University. The DSCs enhanced MRI data were transferred along with the anatomic data to an offline workstation. T2*- weighted signal intensity-time curves were derived on a voxel-by-voxel basis. A region of interest (ROI) of 35–80 mm^2 was drawn over the tumor region showing the highest perfusion value in the perfusion maps, avoiding the regions of vessels, calcification, hemorrhage, cyst, and necrosis. Another ROI was drawn over the contralateral normal-appearing white matter (WM). The value of tumor ROI was divided by the value of contralateral normal WM ROI to estimate normalized tumoral blood flow (nTBF) and normalized tumoral blood volume (nTBV) values based on the rCBF and rCBV maps. High-resolution 3D T1WI with contrast.

Perfusion-weighted imaging color maps post-processing

Included lesions analysis was based on the automatic creation of quantitative perfusion and cerebral blood flow (CBF) maps from each patient after 3D PCASL data, anatomic data & DSC perfusion data were moved to an offline workstation. ROI of 35–80 mm^2 was drawn over the tumor solid part with the highest perfusion value in the color maps. Another ROI was drawn over the contralateral normal-appearing WM. The value of tumor ROI was divided by the value of contralateral normal WM ROI to estimate relative perfusion values.

.For DSC perfusion T2*- weighted signal intensity-time curves were derived on a voxel-by-voxel basis. The final histopathology diagnosis was confirmed by stereotactic biopsy or surgical debulking.

Statistical analysis

Statistical analysis was done by SPSS v27 (IBM©, Chicago, IL, USA). The Shapiro-Wilks test and histograms were used to evaluate the normality of the distribution of data. Quantitative parametric data were presented as mean and standard deviation (SD) and were analyzed by ANOVA (F) test with post hoc test (Tukey). Quantitative non-parametric data were presented as the median and interquartile range (IQR) and were analyzed by the Kruskal-Wallis test with the Mann Test to compare each group. Qualitative variables were presented as frequency and percentage (%) and were analyzed utilizing the Chi-square test. Correlation between various variables was done using the Pearson moment correlation equation. Roc curve was used for the evaluation of diagnostic performance sensitivity, specificity, positive predictive value (PPV), and negative predictive value (NPV). A two-tailed P value < 0.05 was considered statistically significant.

3. RESULTS

Demographic data, cause of referral, clinical presentation, and sex of GBM patients were enumerated in **table 1**.

Table 1: Distribution of the studied patients regarding demographic data, cause of referral, clinical presentation, and sex of GBM patients

		N=40
Age (years)		47±15.2
Sex	**Male**	26(65.0%)
	Female	14(35.0%)
Cause of referral	**Preoperative grading**	21(52.5%)

	Follow up	19(47.5%)
Clinical presentation	**Motor affection**	8(20.0%)
	Decreased orientation	8(20.0%)
	Persistent headache	7(17.5%)
	Seizures	6(15.0%)
	Depression	6(15.0%)
	Sensory affection	5(12.5%)
	Speech affection	5(12.5%)
	Anxiety	3(7.5%)
		N=16
Sex of GBM patients	**Males**	10(62.5%)
	Females	6(37.5%)

Data are presented as mean ± SD or frequency (%). GBM: glioblastoma multiforme.

Age was significantly different between IDH wild multiforme cases and other glioma grades of the studied groups (P <0.05). ASL (CBF) was significantly different between low-grade gliomas and IDH wild glioblastoma, between primary IDH wild glioblasotma and IDH wild glioblastoma residual after radiotherapy and chemotherapy and between post-resection cavity with free resection margin, radiation necrosis and recurrent IDH wild gliobastoma recurrence. **Table 2**

Table 2: Relation between (WHO grade of group (A) and age) and between (final diagnosis and ASL parameters) of the studied patients

	WHO grade			**F**	**P**
	2 (n= 7)	**3 (n= 4)**	**4 (n= 8)**		
Age	33.1±9.5	37.8±9.8	60.6±7	20.885	**<0.001***
	ASL tumoral absolute CBF	**ASL tumoral normalized CBF**			
Pathology					
IDH wild glioblastoma (GBM) (n=11)	113.8[abd]±39.1	2.5±0.7		--	--
Post -resection cavity (n=6)	32[ce]±7.4	0.6±0.2			
Anaplastic astrocytoma grade 3 (n=5)	67[b]±23.6	1.9±0.8			
Oligodendroglioma 1p/19q non codeleted grade 2 (n=5)	51.8±24.4	1.1±0.7			
Astrocytoma grade 2 (n=5)	34.8±10.2	0.8±0.1			
IDH wild glioblastom residual (n=3)	52.7±34.6	1.1±0.6			
Radiation necrosis (n=3)	25.3[ce]±3.1	0.51±0.1			
Pseudo-progression (n=2)	44±0	1±0			
Pleomorphic xanthoastrocytoma grade 2 (n=1[#])	56	2.1			

H(p)	**32.271*(<0.001*)**	**32.505*(<0.001*)**		

Data are presented as mean ± SD.* Significant P value <0.05. F: one-way ANOVA test, H: Kruskal Wallis test, WHO: World Health Organization, ASL: arterial spin-labeling, CBF: cerebral blood flow, IDH: isocitrate dehydrogenase, GBM: glioblastoma multiforme, a: significant with oligodendroglioma grade 2, b: significant with diffuse astrocytoma grade 2, c: significant with anaplastic astrocytoma grade 3, d: significant with GBM residual, e: significant with IDH wild glioblatoma multiforme, #: Excluded from the comparison due to small number of case.

Location, size, conventional MRI, final diagnosis, ASL tumoral absolute CBF, ASL relative CBF, and ASL CBF of the contralateral white matter flow were enumerated in this table. **Table 3**

Table 3: Location and size, conventional MRI, final diagnosis, ASL tumoral absolute CBF, ASL relative CBF, and ASL CBF of the contralateral WM flow of the studied lesions

		N=41
Lesion location	**Parietal**	13(31.7%)
	Temporal	9(21.9%)
	Frontal	7(17%)
	Fronto-parietal	4(9.7%)
	Parieto-temporal	2(4.8%)
	Occipital	3(7.3%)
	Midbrain	2(4.8%)
	Cerebellar and superior cerebellar peduncle	1(2.4%)
Lesion size (cm)		4.1±1.6
Lesion pathology	**IDH wild glioblastoma**	11(26.8%)
	Post resection cavity	6(14.6%)
	Anaplastic astrocytoma grade III	5(12.2%)
	Oligodendroglioma grade II	5(12.2%)
	Astrocytoma grade II	5(12.2%)
	Radiation necrosis	3(7.3%)
	GBM residual	3(7.3%)
	Pseudo-progressions	2(4.8%)
	Pleomorphic xanthoastrocytoma grade 2	1(2.4%)

Data are presented as mean ± SD or frequency (%) or median (IQR). MRI: magnetic resonance imaging, ASL: arterial spin-labeling, CBF: cerebral blood flow, WM: white matter, T2WI: T2 weighted image, IDH: isocitrate dehydrogenase, GBM: glioblastoma multiforme.

There was a significant difference between ASL, DSCE color map, different ASL parameters, DSCE absolute CBF, DSCE regional and relative CBV, and final histopathological grade (P<0.05). There was no significant difference between DSCE relative CBF and final histopathological grade. **Table 4**

Table 4: Relation between final histopathological grade with ASL and DSCE color map, post-treatment outcome, different ASL parameters, and DSCE in the studied lesions

	Final histopathological grade						FET and H	P
	Low grade (n= 11)	High grade (n= 16)	Resection cavity (n= 6)	GBM residual (n= 3)	Radiation necrosis (n= 3)	Pseudo progression (n= 2)		
ASL color map								
Hypo perfused	5(45.5%)	0(0.0%)	6 (100.0%)	2 (66.7%)	3 (100.0%)	1(50.0%)	48.305	**<0.001***
Hyperperfused	0(0.0%)	8(50.0%)	0 (0.0%)	0 (0.0%)	0 (0.0%)	0(0.0%)		
Iso perfused	5(45.5%)	2(12.5%)	0 (0.0%)	0 (0.0%)	0 (0.0%)	1(50.0%)		
The hyperperfused solid part of the tumor with necrotic hypo-perfused part	1(9.1%)	6(37.5%)	0 (0.0%)	1(33.3%)	0 (0.0%)	0(0.0%)		
DSCE Color map								
Hypo perfused	5(45.5%)	0(0.0%)	5 (83.3%)	2 (66.7%)	3 (100.0%)	1(50.0%)	41.949	**<0.001***
Hyperperfused	0(0.0%)	8(50.0%)	0 (0.0%)	0 (0.0%)	0 (0.0%)	1(50.0%)		
Iso perfused	5(45.5%)	2(12.5%)	0 (0.0%)	0 (0.0%)	0 (0.0%)	0(0.0%)		
The hyperperfused solid part of the tumor with necrotic hypo-perfused	1(9.1%)	6(37.5%)	1 (16.7%)	1 (33.3%)	0 (0.0%)	0(0.0%)		
Different ASL parameters								
ASL absolute CBF	40(25–56)	90(44–184)	32.5 (24 – 40)	39 (27 – 92)	26(22 – 28)	44(44–44)	31.996	**<0.001***
ASL relative CBF	0.9(0.5–2.1)	2.2(0.7–3.8)	0.7 (0.4 – 0.8)	1.1 (0.5 – 1.7)	0.5(0.4 – 0.5)	1(1–1)	29.593	**<0.001***
DSCE								
DSCE absolute CBF	35(5–70)	60.5(20–188)	21 (10 – 25)	34 (30 – 57)	22(6–22)	35(35–35)	21.065	**0.001***
DSCE relative CBF	1(0.5–3)	2.8(1.5–3.3)	0.9 (0.3 – 1.3)	1.2 (0.6 – 1.7)	0.3(0.3–0.6)	5(5–5)	8.531	0.129
DSCE regional CBV	1.2(0.4–4.6)	4.5(2.1–17)	1.3 (0.4 – 3.8)	1.7 (0.7 – 4.9)	0.6(0.3–0.7)	8(8–0.8)	25.411	**<0.001***
DSCE relative CBV	1.1(0.6–2.5)	2.4(1.1–6.4)	0.8 (0.3 – 3.1)	1.7 (0.4 – 1.9)	0.5(0.2–0.5)	6.2(6.2-0.6)	23.692	**<0.001***

Data are presented as frequency (%) or median (IQR). * Significant P value <0.05. FET: fisher exact test, H: Kruskal Wallis test, ASL: arterial spin-labeling, DSCE: dynamic susceptibility contrasts enhanced perfusion, GBM: glioblastoma multiforme, CBF: cerebral blood flow, PWI: perfusion-weighted imaging, CBV: cerebral blood volume.

All ASL perfusion parameters showed a significant difference (P < 0.001) between low- and high-grade gliomas, both ASL rCBF and ASL tCBF values showed a sensitivity of 91.97%, specificity of 90.91%, NPV of 90.9%, PPV of 91.7% with AUC for ASL-CBF 0.962 and confidence interval 0.894-1. ASL-rCBF and ASL-PWI respectively, AUC= 0.909 and 0.977 with confidence intervals of 0.771-1.0 and 0.925-1.0, PPV of 90.5% and 92.3% and NPV of 96.3% and 100%, cutoff value of high-grade glioma for rCBF was more than 1.1and 500. All DSC perfusion parameters showed a statistically significant value in the discrimination of low- and high-grade gliomas. DSC-CBF, rCBF, rCBV, and regional CBV respectively showed AUC= 0.818, 0.939, 0.932 and0.883 with a confidence interval of 0.643-0.994, 0.821-1.0, 0.832-1.0 and 0.746-1.0 sensitivity of 83.33%,100%, 91.67% and 83.33 % specificity of 63.64%,90.9%, 81.82 % and 72.7 %, PPV of 71.4%,92.3%, 84.6 % and76.9% and NPV of 77.8%, 100 %,90% and 80%. **Figure 1**

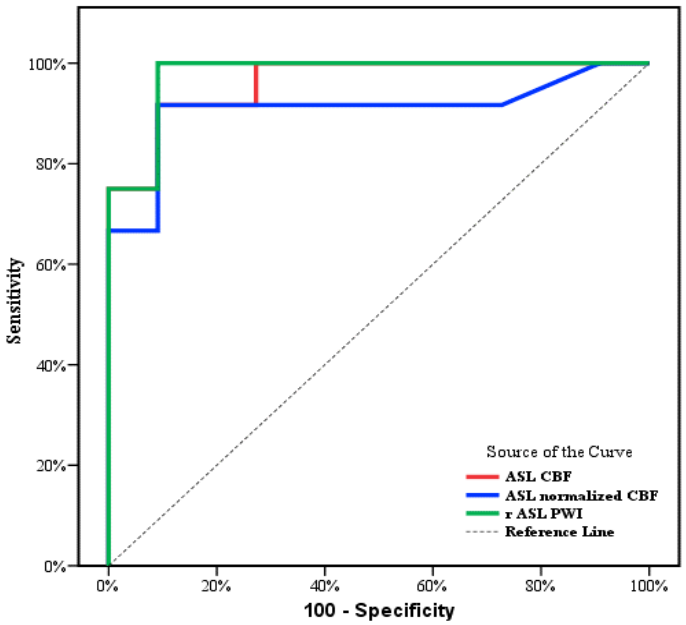

Figure (1): ROC curve for ASL to discriminate high grade from low grade gliomas

There was a highly strong correlation between (ASL-tCBF and absolute DSC -tCBF and DSC -tCBV), between (ASL rCBF, DSC rCBF, and DSC rCBV). There was a significant agreement was present between ASL relative ASL perfusion weighted image signal and dynamic contrast-enhanced relative CBV. **Figure 2**

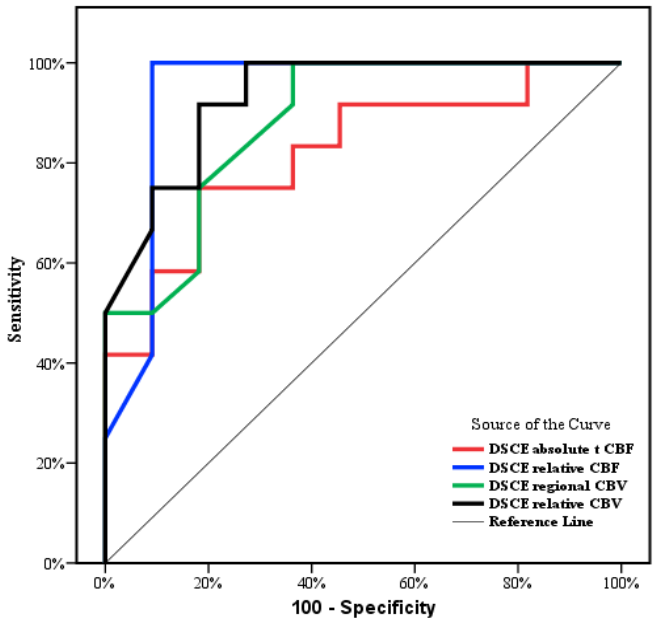

Figure (2): ROC curve for DSCE to discriminate high grade from low grade gliomas

T1 post-contrast images showed less sensitivity, specificity, NPV, PPV, and accuracy compared to ASL perfusion parameters. **Table 5**

Case 1: A 67-year-old hypertensive female patient, presented clinically with disturbed conscious level, headache, dysarthria, and dizziness 2 months ago with intact motor functions. MRI diagnosis: high-grade glioma with peri-lesional infiltration - Multiforme/IDH wild type. Final histopathological diagnosis by debulking biopsy: grade IV GBM, IDH wild type. **Figure 3**

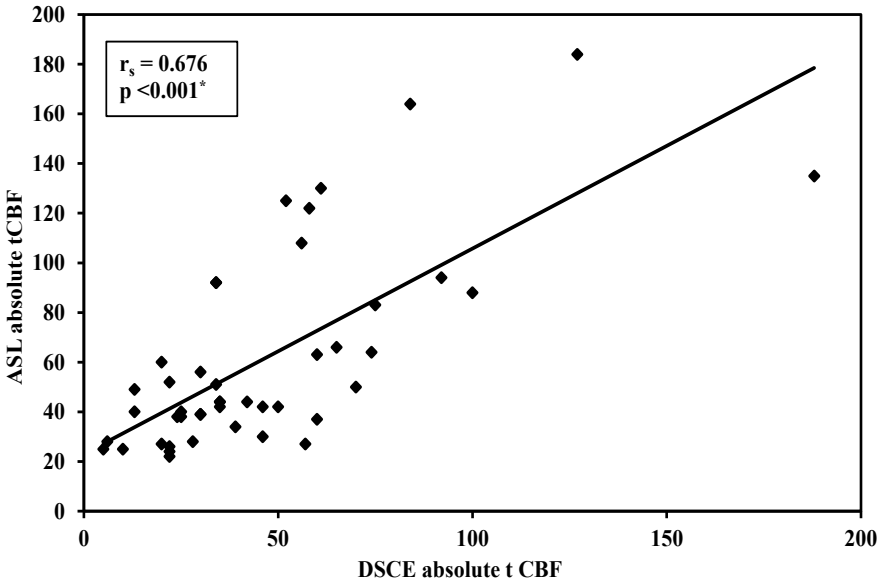

Figure (3): Correlation between ASL absolute tCBF with DSCE absolute t CBF in the studied lesions with glioma (number = 45)

Case 2: A 41-year-old male patient, presented clinically with a progressive course of left sensory affection in the form of tingling and numbness in the left hand together with its weakness. MRI diagnosis: A hemorrhagic low-grade glioma. Final histopathologic diagnosis via de-bulking biopsy: Diffuse gemiocytic astrocytoma, grade II. **Figure 4**

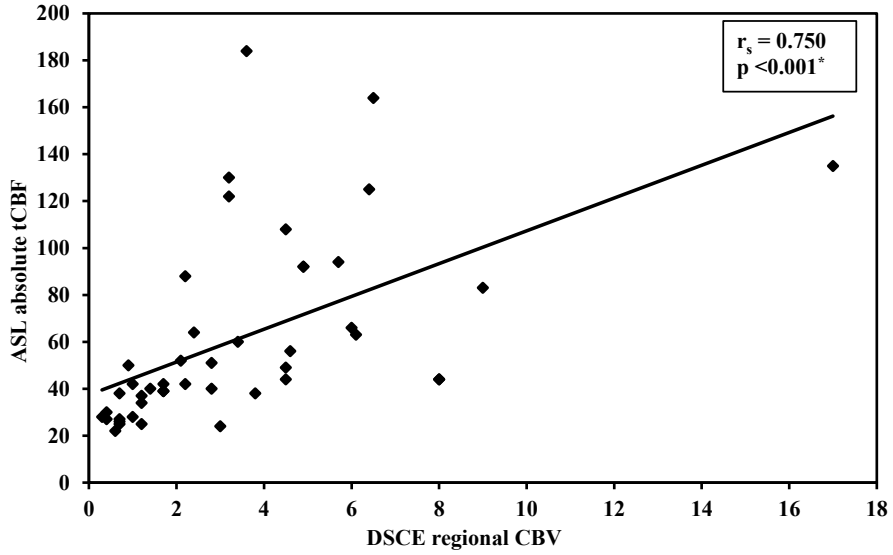

Figure (4): Correlation between ASL absolute tCBF with DSCE regional CBV in the studied lesions with glioma (number = 45)

Case 3: A 23-year-old female patient operated five years ago, biopsy proven astrocytoma grade II. She received chemotherapy with post-operative MRI revealed an area of encephalomalacia. She developed new symptoms of progressive

left side weakness affecting arms and legs. Clinical examination revealed poor hand grip, weak resistance against forced flexion and extension of upper and lower limbs. MRI diagnosis showed recurrent two intra axial right fronto-parietal lesions with perfusion values suggesting high grade lesions. Right parietal area of encephalomalcia with clear operative margins. Final histo-pathological diagnosis of the newly discovered lesions showed anaplastic astrocytoma grade III. **Figure 5**

Case 4: A 50-year-old male patient aged, 1st diagnosed at 2018, presented by headache, drowsiness, and single convulsion attack, no motor or sensory weakness,1st operation done at 2018 pathologically proven to be oligodendroglioma grade III, received chemotherapy. He came for follow up. MRI diagnosis showed conventional and perfusion MRI findings are in favor of the right parietal area of radiation necrosis confirmed by biopsy. **Figure 5**

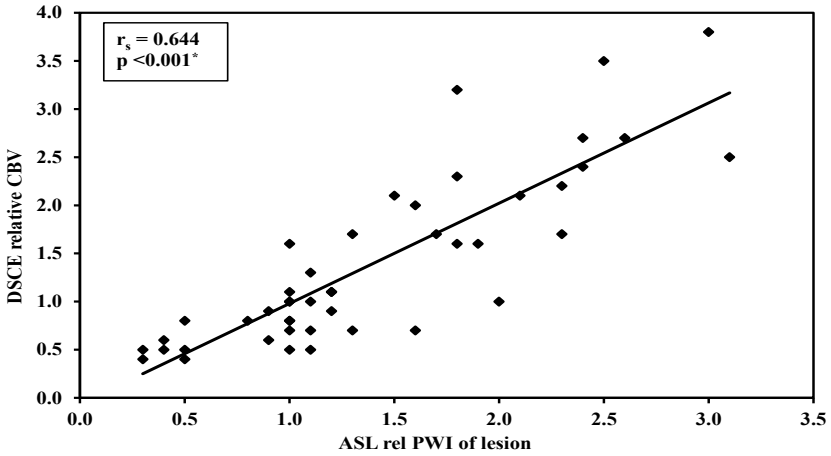

Figure (5): Correlation between DSCE relative CBV and ASL relative PWI of lesion (n= 45)

4. DISCUSSION

Brain gliomas which represent about 28% of all brain tumors contribute to significant morbidity, mortality, and a huge loss in terms of productivity and quality of life with no age group immune to it. [11]

In the present study, the most affected brain lobes were the parietal lobes followed by temporal lobes. In line with our study, **Mohammadi et al.** [12] demonstrated that the left parietal lobe of the cerebrum was the most affected cerebral lobe with a percentage of 18.9% of included lesions.

This study showed agreement between the qualitative ASL and DSCE color maps in differentiation between high and low-grade gliomas (P<0.001), in agreement with our results, ELbehiery et al. [13] found that high grade gliomas in their study were hyper-perfused in ASL color maps. This is explained by the malignant histopathological feature of disorganized, irregular neo-vascular channels with shunting which results in increased perfusion. **Bayraktar et al.**[14] compared both ASL and DSC color maps and found that ASL color maps were more specific than DSC color maps.

The current study ROI placement was in the solid part of tumor mass using post-contrast images. Then ROI was transcribed on perfusion maps and afterward, mean TBF was measured at ASL and DSC color maps, with normalization of CBF value to contra-lateral WM this method of ROI analysis. Meanwhile, **Brendle et al.** [15] used a large ROI covering almost all the solid tumor based on FLAIR image to measure TBF.

Our study showed that ASL parameters were significantly correlated to the final pathology of included lesions, this came in agreement, with **Youssef et al.** [16] who found that the lowest ASL CBF was 5 mL/100gm/min, and the maximum was 105 in 55 space-occupying lesions. **Batalov et al.** [17] found that relative ASL CBF and absolute CBF values in grade 2 gliomas are 36.5±15.5 ml/100 gm/min with a relative tumoral CBF value of 2.3± 1. **Zeng et al.** [18] studied five cases of Grade 2 astrocytoma, with mean absolute tumoral ASL CBF 75.4 ± 10 ml/100 gm/min with mean ASL normalized tumoral CBF ASL rCBF 0.9±0.18.

In the current study both astrocytoma and oligodendroglioma grade II showed lower ASL t-CBF and ASL r-CBF when compared to IDH wild glioblastoma ASL perfusion values this comes in line with, **Alsaedi et al.** [19] in their study.

However, In the current study no significant difference between grades 3 &4 as regards absolute CBF values, this was against **Batalov et al.** [17] who observed a significant difference between grade 3 and grade 4 glioma ASL perfusion parameters.

As regards ASL use in monitoring the treatment response of GBM lesions, the included residual GBM lesions after chemoradiotherapy showed a mean tumoral ASL value of 52.7 ± 34.6 ml/100gm/min, mean relative ASL CBF value of 1.1 ± 0.6, with a decrease in the mean cerebral flow of the included residual glioblastoma lesions at time of initial diagnosis.

Supporting our results **Petr et al.** [20] found a significant decrease in perfusion parameters compared to the pre-treatment baseline value of GBM.

In agreement with the current study, ROC curves results support the role of ASL perfusion as a good alternative to DSC enhanced perfusion in discriminating high-grade from low-grade gliomas, **Guo et al.** [21] found out that ASL-CBF means and ASL-CBF maximum values are significantly lower in the LGGs than those in HGGs. Supporting our results, **Wang et al.** [22] found that ASL absolute TBF showed a specificity of 89.3% and ASL rTBF showed a sensitivity of 96.4% when discriminating LGG and HGG using a ROC curve. **Patil et al.** [23] found that the least specific perfusion is the regional DSC CBF with specificity of 62.5% and the least sensitive value is the regional DSC CBV with sensitivity of 72%.

Using Spearman correlation, the current study found very good agreement between ASL and DSCE perfusion parameters with an R-value of 0.67, and 0.7 for different perfusion parameters this agreed with **Arisawa et al.** [24] with r value of 0.767 between DSCE- rCBF and ASL- rCBF, r value of 0.847 between ASL-rCBF and DSC- rCBV. Additionally, **Patil et al.** [23] found a strong correlation between both ASL and DSC perfusion parameters and suggested that both are effective in differentiating low- and high-grade gliomas.

In the current study recurrent IDH wild glioblastoma ASL parameters were higher when compared to radiation necrosis ASL parameters, this is supported by **SU et al.** [25] **&Nguyen et al.** [26] who found a significant difference between ASL perfusion parameters of recurrent high-grade gliomas and radiation necrosis. We suggest the use of ASL perfusion as a good alternative to DSC perfusion as a routine part of brain MRI protocol for space-occupying lesions in the brain as it's safer for the patient with no gadolinium injection and also can be used in follow-up the lesion perfusion response to chemoradiotherapy.

Conclusions:

Magnetic resonance ASL perfusion shows good agreement with DSC perfusion in discriminating low from high-grade gliomas and in following up treatment response of high-grade gliomas to treatment with the advantage of being without contrast injection which offers a good alternative for DSC perfusion in patients with contraindication to contrast injection, also can be a promising non expensive primary perfusion technique in developing countries.

Case (No.1)

A 67-year-old hypertensive female patient, presented clinically with disturbed conscious level, headache, dysarthria and dizziness 2 months ago with intact motor functions.

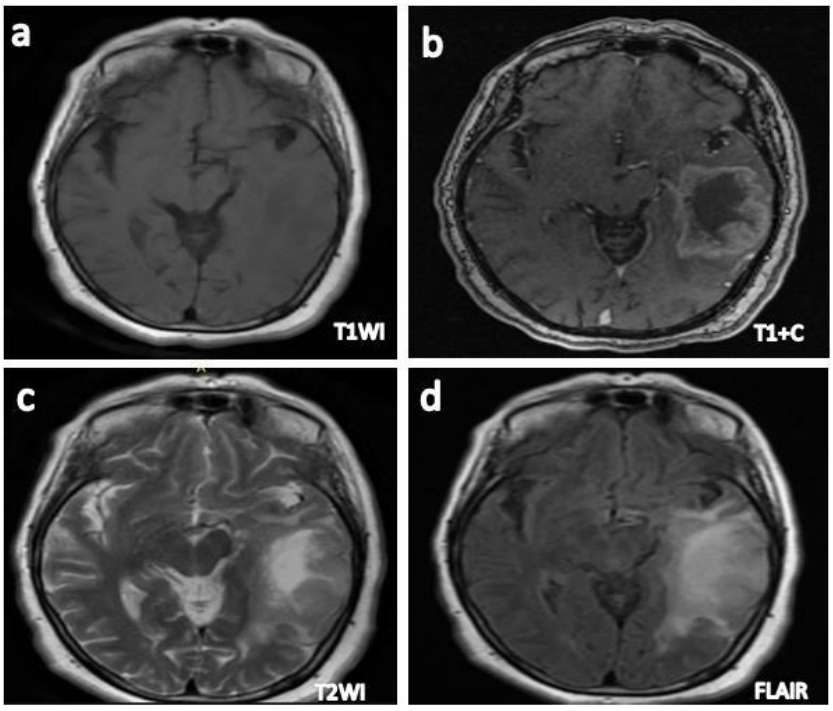

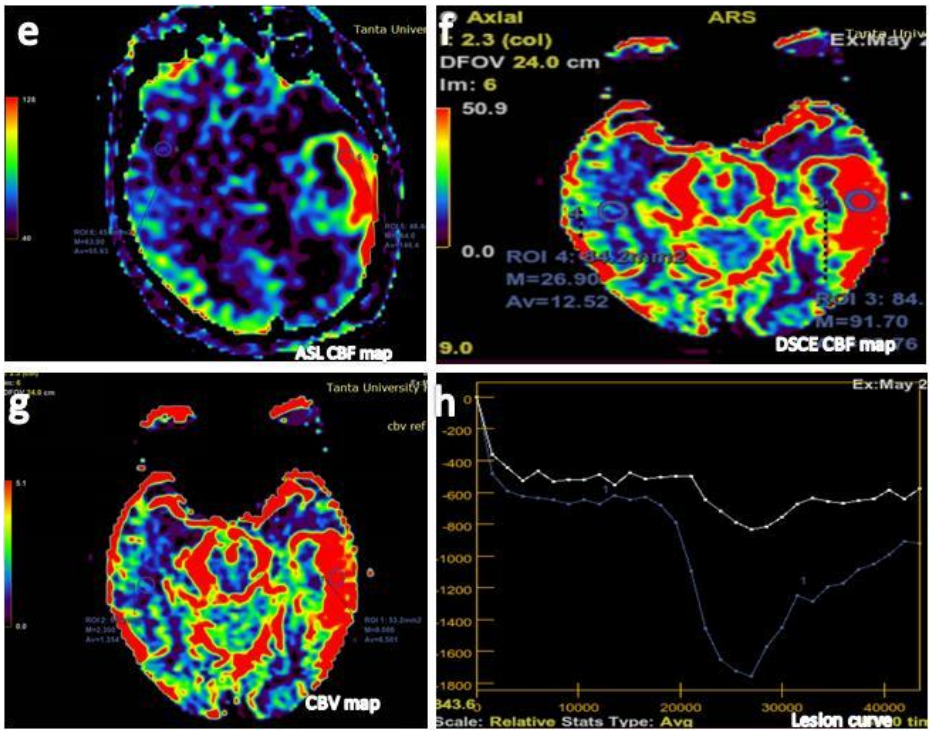

Figure (53): MRI of the brain(axial views) shows an ill -defined non-hemorrhagic intraaxial SOL in the left temporo-occipital lobes, displaying a low signal on T1WI , measuring about 5x4 x5 cm in its maximum dimensions with marginal uneven enhancement and central area of cystic degeneration (a,b) , high signal on T2WI and FLAIR sequence, being surrounded by a vasogenic edema and both exert mass effects in the form of effacement of overlying cortical sulci and compression of the temporal horn of left lateral ventricle(c,d). **ASL and DSC color maps show** marked hyperperfusion of the lesion mild extending to the peri-lesional area and hypoperfused its central necrotic part compared with the contralateral normal white matter. **ASL r CBF=3.5, CBF absolute value = 160 ml/100 gm/min,DSC r CBF =3.5 , DSC CBF absolute value = 75 ml/100 gm/min , DSC rCBV = 3.4(e-g). The lesion signal to time curve shows rapid signal drop to baseline and rapid rise (blue curve in h).**

MRI diagnosis: High grade glioma with peri-lesional infiltration -Multiforme/IDH wild type.

Final histopathological diagnosis by debulking biopsy :Grade IV glioblastoma multiforme, +ve for IDH mutation.

Case (No.2)

A 50-year-old male patient, presented clinically with persistent headache, hand tremors, right eye twitches , amnesia , anxiety and loss of appetite. He was under radiotherapy on top of a histologically -proven anaplastic astrocytoma grade III and mandatory GBM transformation.

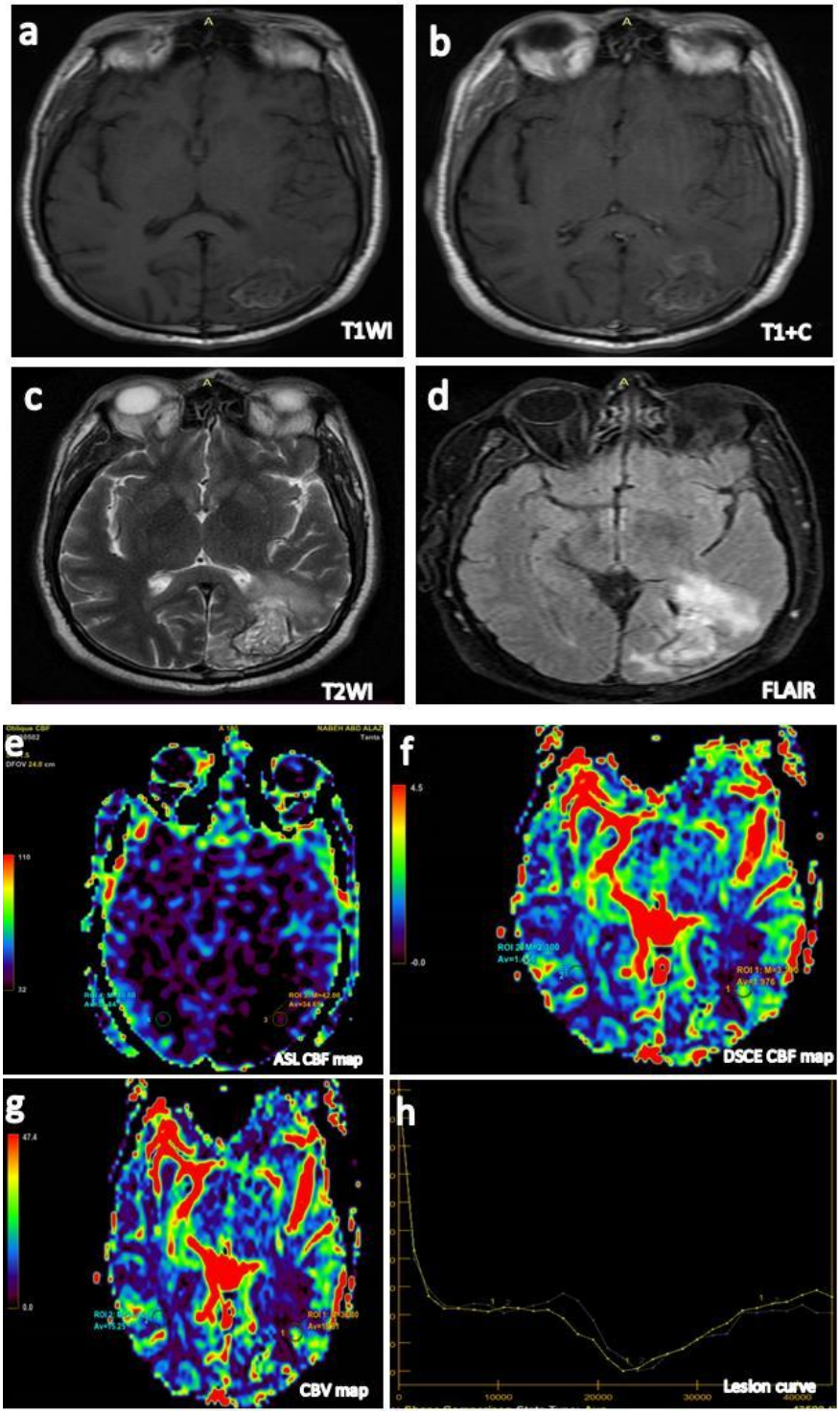

Figure (54a): Post- radiotherapy MRI of the brain(axial views) shows an ill-defined hemorrhagic mildly-enhancing intraaxial SOL in the left occipital lobe, displaying high signal on T1WI,measures about 3.7 x 2.3 cm in its maximum dimensions , high signal on T2WI and FLAIR sequence and is surrounded by mild perifocal edema, both exert mass effects with effacement of the overlying cortical sulci and attenuation of the occipital horn of left lateral ventricle and the lesion shows a signal void hemosedrin rim in all sequences(a-d). **ASL and DSC color maps** show a hypoperfused lesion in comparison with the contralateral brain white matter with **ASL r CBF=1.1, ASL CBF absolute value = 40 ml /100 gm/min, DSC r CBF =1.1, DSC CBF absolute value = 29 ml/100 gm/min, DSC rCBV =0.7(e-g) and the lesion signal to time curve shows signal changes similar to that of the contralateral normal brain white matter (yellow and blue curve in h respectively).**

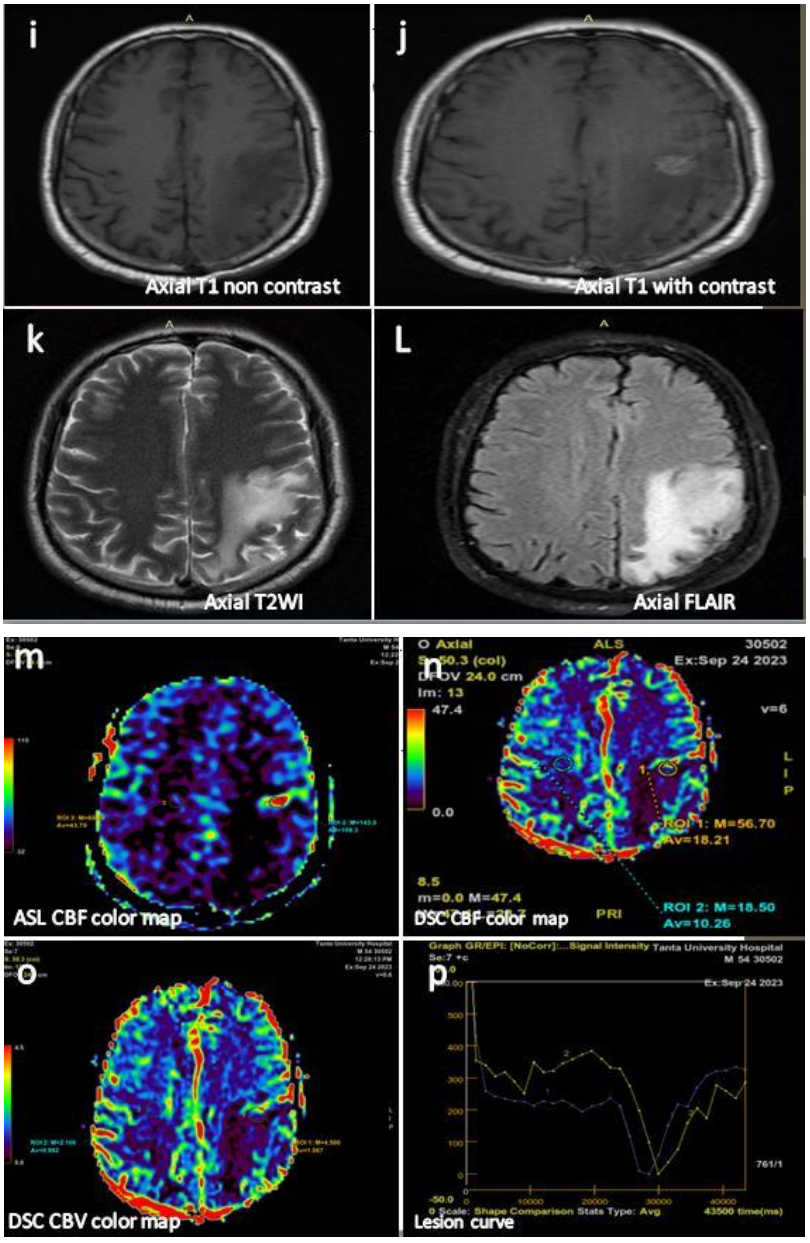

Figure (54b): Higher axial MRI cuts of the brain in the same patient show another newly-developed enhancing non-hemorrhagic lesion in the left parietal lobe,displaying low signal on T1WI ,high signal on T2WI and FLAIR sequence ,measuring about 1.6 x1.5 cm in its maximum dimensions with extensive peri-focal edema and both extert mass effects in the form of effacement of the overlying cortical sulci (i-l). **ASL and DSC color maps** show a hyperperfused lesion in comparison with the contralateral normal brain white matter. **ASL r CBF=1.1, ASL CBF absolute value = 143 ml /100 gm/min, DSC r CBF =2.9, DSC CBF absolute value = 56 ml/100 gm/min, DSC r CBV =2.7(m-o)** and the lesion signal to time curve shows rapid signal drop and peaking with rapid upward rise compared to contralateral white matter curve(yellow and blue curve in p respectively).

MRI diagnosis: Bifocal gliomas with a stationary size of the original lesion and its perfusion values downgrading into low grade lesion and another newly -developped lesion with its perfusion values in favor of a high grade glioma.

-Final diagnosis of the newly-developed lesion through a stereotactic biopsy: An anaplastic astrocytoma , grade III with inevitable GBM transformation.

Acknowledgements: Nil

REFERENCES

[1] Qu Y, Kong D, Wen H, Ou X, Rui Q, Wang X, et al. Perfusion measurement in brain gliomas using velocity-selective arterial spin labeling: comparison with pseudo-continuous arterial spin labeling and dynamic

susceptibility contrast MRI. Eur J Radiol. 2022;32:2976-87.

[2] McKinnon C, Nandhabalan M, Murray SA, Plaha P. Glioblastoma: clinical presentation, diagnosis, and management. BMJ. 2021;374:200-30.

[3] Blionas A, Giakoumettis D, Klonou A, Neromyliotis E, Karydakis P, Themistocleous MS. Paediatric gliomas: diagnosis, molecular biology and management. Ann Transl Med. 2018;60:400-30.

[4] Verburg N, de Witt Hamer PC. State-of-the-art imaging for glioma surgery. Neurosurg Rev. 2021;44:1331-43.

[5] Nilsen LB, Emblem KE. Magnetic resonance imaging for quantification of brain vascular perfusion. Brain Tumors. 2021;30:289-321.

[6] Ninatti G, Sollini M, Bono B, Gozzi N, Fedorov D, Antunovic L, et al. Preoperative [11C] methionine PET to personalize treatment decisions in patients with lower-grade gliomas. Neuro-oncol. 2022;24:1546-56.

[7] Castellano A, Bailo M, Cicone F, Carideo L, Quartuccio N, Mortini P, et al. Advanced imaging techniques for radiotherapy planning of gliomas. Cancers. 2021;13:10-63.

[8] Abdelgawad MS, Kayed MH, Reda MIS, Abdelzaher E, Farhoud AH, Elsebaie N. Contribution of advanced neuro-imaging (MR diffusion, perfusion and proton spectroscopy) in differentiation between low grade gliomas GII and MR morphologically similar non neoplastic lesions. EJNM. 2022;53:20-6.

[9] Anzalone N, Castellano A, Cadioli M, Conte GM, Cuccarini V, Bizzi A, et al. Brain gliomas: multicenter standardized assessment of dynamic contrast-enhanced and dynamic susceptibility contrast MR images. J Radiol. 2018;287:933-43.

[10] Waqar M, Lewis D, Agushi E, Gittins M, Jackson A, Coope D. Cerebral and tumoral blood flow in adult gliomas: a systematic review of results from magnetic resonance imaging. Br J Radiol. 2021;94:30-5.

[11] Weller M, Wick W, Aldape K, Brada M, Berger M, Pfister SM, et al. Glioma. Nat Rev Dis. 2015;10:1-18.

[12] Mohammadi E, Moghaddam SS, Azadnajafabad S, Maroufi SF, Rashidi MM, Naderian M, et al. Epidemiology of brain and other central nervous system cancers in the north africa and middle east region: a systematic analysis of the global burden of disease study 1990-2019. World Neurosurg. 2023;171:796-819.

[13] ElBeheiry AA, Emara DM, Abdel-Latif AA-B, Abbas M, Ismail AS. Arterial spin labeling in the grading of brain gliomas: could it help? EJNM. 2020;51:1-11.

[14] Bayraktar ES, Duygulu G, Çetinoğlu YK, Gelal MF, Apaydın M, Ellidokuz H. Comparison of ASL and DSC perfusion methods in the evaluation of response to treatment in patients with a history of treatment for malignant brain tumor. BMC Med Imaging. 2024;24:70-60.

[15] Brendle C, Hempel JM, Schittenhelm J, Skardelly M, Tabatabai G, Bender B, et al. Glioma grading and determination of IDH mutation status and ATRX loss by DCE and ASL perfusion. Clin Neuroradiol. 2018;28:421-8.

[16] Youssef A, Al Neikedy A, Khater H, Hanora M. Role of arterial spin labelling cerebral perfusion in assessment of different intra cranial disorders (using 3 Tesla MRI). BJAS. 2021;6:333-41.

[17] Batalov AI, Zakharova NE, Pronin IN, Belyaev AY, Pogosbekyan EL, Goryaynov SA, et al. 3D pCASL-perfusion in preoperative assessment of brain gliomas in large cohort of patients. Sci Rep. 2022;12:21-2.

[18] Zeng Q, Jiang B, Shi F, Ling C, Dong F, Zhang J. 3D pseudocontinuous arterial spin-labeling MR imaging in the preoperative evaluation of gliomas. AJNR Am J Neuroradiol. 2017;38:1876-83.

[19] Alsaedi A, Doniselli F, Jäger HR, Panovska-Griffiths J, Rojas-Garcia A, Golay X, et al. The value of arterial spin labelling in adults glioma grading: systematic review and meta-analysis. Oncotarget. 2019;10:15-89.

[20] Petr J, Platzek I, Seidlitz A, Mutsaerts HJ, Hofheinz F, Schramm G, et al. Early and late effects of radiochemotherapy on cerebral blood flow in glioblastoma patients measured with non-invasive perfusion MRI. Radiother Oncol. 2016;118:24-8.

[21] Guo D, Jiang B. Noninvasively evaluating the grade and IDH mutation status of gliomas by using mono-exponential, bi-exponential diffusion-weighted imaging and three-dimensional pseudo-continuous arterial spin labeling. Eur J Radiol. 2023;160:110-721.

[22] Wang YL, Chen S, Xiao HF, Li Y, Wang Y, Liu G, et al. Differentiation between radiation-induced brain injury and glioma recurrence using 3D pCASL and dynamic susceptibility contrast-enhanced perfusion-weighted imaging. Radiother Oncol. 2018;129:68-74.

[23] Patil V, Malik R, Sarawagi R. Comparative study between dynamic susceptibility contrast magnetic resonance imaging and arterial spin labelling perfusion in differentiating low-grade from high-grade brain tumours. Pol J Radiol. 2023;88:521-8.

[24] Arisawa A, Watanabe Y, Tanaka H, Takahashi H, Matsuo C, Fujiwara T, et al. Comparative study of pulsed-continuous arterial spin labeling and dynamic susceptibility contrast imaging by histogram analysis in evaluation of glial tumors. Neuroradiol. 2018;60:599-608.

[25] Su H, Kong X, Su S, Wu K, Shi H. The value of arterial spin labeling and dynamic susceptibility contrast in the differential diagnosis of the recurrence of glioma. Invest Clin. 2020;61:949-57.

[26] Nguyen TB, Zakhari N, Velasco Sandoval S, Guarnizo-Capera A, Alexios Gulak M, Woulfe J, et al. Diagnostic accuracy of arterial spin-labeling, dynamic contrast-enhanced, and DSC perfusion imaging in the diagnosis of recurrent high-grade gliomas: a prospective study. AJNR Am J Neuroradiol. 2023;44:134-42.